



Compact MR-compatible ergometer and its application in cardiac MR under exercise stress: A preliminary study

Bo He^{1,2} | Yushu Chen¹ | Lei Wang^{1,2} | Yang Yang³  | Chunchao Xia¹ | Jie Zheng⁴ | Fabao Gao^{1,2} 

¹Department of Radiology, West China Hospital of Sichuan University, Chengdu, Sichuan, China

²Molecular Imaging Center, West China Hospital of Sichuan University, Chengdu, Sichuan, China

³Icahn School of Medicine at Mount Sinai, New York, New York, USA

⁴Mallinckrodt Institute of Radiology, Washington University in St Louis, St. Louis, Missouri, USA

Correspondence

Fabao Gao, Department of Radiology and Molecular Imaging Center, West China Hospital of Sichuan University, 37 Guoxue Alley, Chengdu, Sichuan 610041, China. Email: gaofabao@wchscu.cn

Funding information

National Natural Science Foundation of China, Grant/Award Numbers: 81930046, 81829003; The Expert Workstation of Yunnan Province, Grant/Award Number: 202105AF150037

Purpose: To develop a compact MR-compatible ergometer for exercise stress and to initially evaluate the reproducibility of myocardial native T1 and myocardial blood flow (MBF) measurements during exercise stress performed on this ergometer.

Methods: The compact ergometer consists of exercise, workload, and data processing components. The exercise stress can be achieved by pedaling on a pair of cylinders at a predefined frequency with adjustable resistances. Ten healthy subjects were recruited to perform cardiac MRI scans twice in a 3.0T MR scanner, at different days to assess reproducibility. Myocardial native T1 and MBF were acquired at rest and during a moderate exercise. The reproducibility of the two tests was determined by the intra-group correlation coefficient (ICC) and coefficient of variation (CoV).

Results: The mean exercise intensity in this pilot study was 45 Watts (W), with an exercise duration of 5 min. Stress induced a significant increase in systolic blood pressure (from 113 ± 11 mmHg to 141 ± 12 , $P < 0.05$) and maximal increase in heart rate by $74 \pm 19\%$. The rate pressure product increased two-fold ($P < 0.001$). Excellent reproducibility was demonstrated in native T1 during the exercise (CoV = 3.0%), whereas the reproducibility of MBF and myocardial perfusion reserve during the exercise was also good (CoV = 10.7% and 8.8%, respectively).

Conclusion: This pilot study demonstrated that it is possible to acquire reproducible measurements of myocardial native T1 and MBF during the exercise stress in healthy volunteers using our new compact ergometer.

KEYWORDS

cardiac MR, exercise stress, MR-compatible pedal exercise, native T1, perfusion

1 | INTRODUCTION

For patients with various cardiac diseases, e.g., the valvular heart disease,¹ congenital heart disease² and coronary artery disease (CAD) detection,³ stress cardiac imaging is often used as an important tool to detect underlying pathology that may not manifest at rest.^{4,5} It has been well acknowledged that cardiovascular MR (CMR) can accurately and reproducibly assess myocardial anatomy, function, tissue characteristics, and vasculature without exposure to radiation, and has great potentials for clinical diagnosis of cardiac diseases.^{6,7} In stress CMR, pharmacologically induced stress by the infuse of adenosine or dobutamine remains the most widely available stress approach.⁸ However, physical exercise is known to have a higher sensitivity and better safety profile to provide functional state and hemodynamic response, and has fewer adverse events compared to pharmacological stressors.^{9,10} As such, current guidelines advise physical exercise as the preferred method for stress imaging when feasible.^{11,12}

While several exercise approaches for CMR study have been well developed for clinical research, including exercise on a MR-compatible treadmill adjacent to an MR scanner,^{13–15} in-scanner supine cycle ergometer,^{4,16} and supine stepper-stress,¹⁷ Exercise CMR (Ex-CMR) is not widely used in clinical practice. Treadmill Ex-CMR is currently the only Ex-CMR modality to demonstrate clinical utility in ischemia detection of CAD patients.¹⁵ However, the relatively large variability in heart rate and blood pressure after the treadmill exercise may limit its clinical assessment. In-scanner Ex-CMR with a supine cycle or stepper ergometers overcomes this issue, but CMR scanning suffers from increased bulk body motion and respiratory motion, particularly when workload increases.¹⁸ Other important limitations of these commercial exercise systems are relatively large device sizes (less convenient for transportation, storage, and placement on an MR table) and high cost.

Therefore, the objective of this study was to: (1) develop a low-cost and compact MR-compatible supine pedal exercise ergometer; (2) demonstrate its feasibility and reproducibility to induce exercise stress for Ex-CMR in 10 healthy subjects.

2 | METHODS

2.1 | Study population

Ten healthy volunteers (5 males and 5 females) were recruited in this prospective pilot study (mean age = 25.7 ± 1.8 y; mean weight = 61.5 ± 5.4 kg; mean height = 167.3 ± 10.2 cm; maximal height = 183 cm;

maximal body mass index (BMI) = 26.85). All subjects were medically healthy and none of them had a history of cardiovascular pulmonary or renal disease, as determined by physical and neurological examination and laboratory tests. All the participants underwent the Ex-CMR test and retest (at least 5 days apart between test and retest). The study was approved by the ethics committee of the local institute and written informed consent was given by the volunteers prior to the first study.

2.2 | MR-compatible ergometer

2.2.1 | Mechanical design

The ergometer consists of exercise (piston cylinder apparatus, sponge pads, etc.), workload (electronic and gas source control modules to control air pressure within the piston cylinder), and data processing components (Figure 1A). The materials used include high-density rubber, aluminum alloy, nylon, etc., all of which are compatible with 3T MR scanners. The exercise component dimensions were 450 mm in width, 600 mm in length, and 300 mm in height, whereas the weight is 25 kg and the maximum static load is 200 kg. The entire ergometer system can be stored in a compact container for easy transportation (Figure 1B). The base of the exercise component is a 1.27 cm (1/2 in.) thick HDPE sheet, with two sponge pads placed on. These base and sponge pads allow both the device and subject to slide on the MR table as needed to ensure the torso is inside the MR bore while the legs are free to move.

The pedaling motion is accomplished through the use of two piston cylinder apparatuses which is composed of a foot pedal, a cylinder fixing plate, a plastic bearing, an air cylinder, a foot pedal, and a pedal slide rail. Structurally, the air cylinder is composed of a cylinder tube, a cylinder head, a piston, a piston rod, and a cylinder damper (Figure 1C). One foot pedal is 25.40 cm (10 in.) in length, 12.7 cm (5 in.) in width, and 1.27 cm (1/2 in.) in thickness. To reduce bulk movement by the subject, a nylon belt, horizontal bars, and a shoulder harness are used to secure the subject to the device (Figure 1D). The shoulder harness and nylon belt have quick releasing clips that allow the subject to be removed quickly in case of a medical emergency.

2.3 | Air pressure adjustment components and data processing components

The resistance of the equipment can be adjusted (0–5 bar) by the workload component through the pressurized

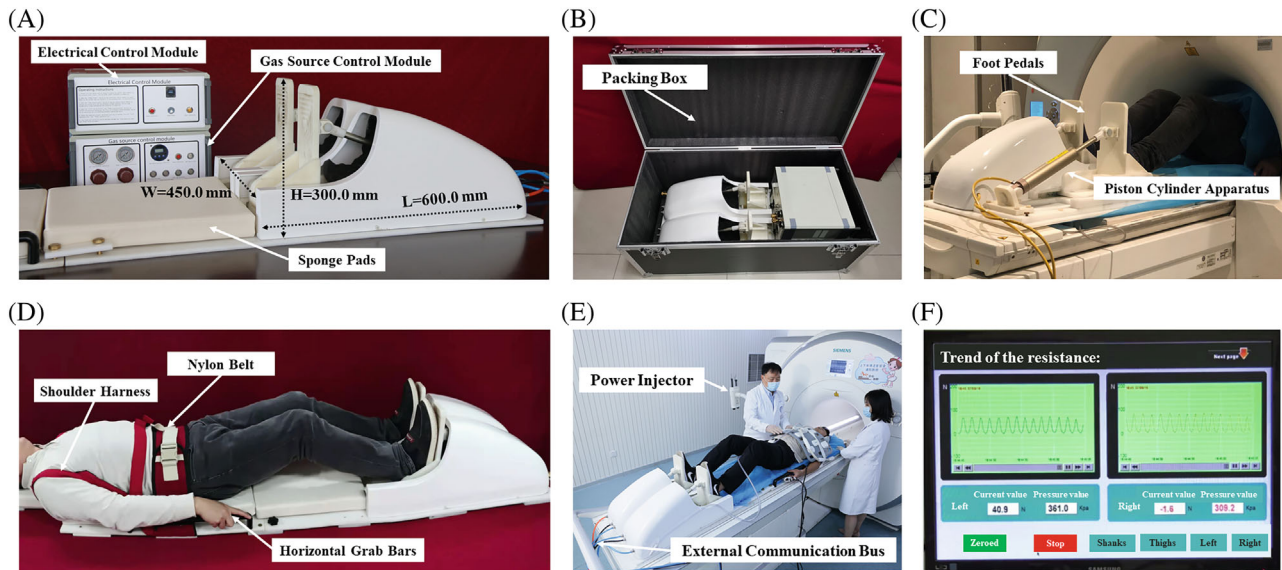


FIGURE 1 General view and the experimental demonstration of the MR-compatible pedal ergometer. A, The ergometer consists of motion components, air pressure adjustment components and data processing components with relatively small size (height = 300 mm, width = 450 mm, length = 600 mm). B, The device can be placed in one packing box. C, Piston cylinder apparatus is composed of a cylinder tube, a cylinder head, a piston, a piston rod and a cylinder damper. D, A nylon belt, horizontal bars, and a shoulder harness are used to secure the subject to the device to reduce bulk movement. E, Healthy subject protocol and supine pedal exercise was performed with a customer-made MR-compatible ergometer onto the MR Table. F, The workload was measured and displayed by monitors in real time (F).

airway. The current design can provide a wide range of resistance suited to subjects with different ages, muscle strength, and health status. Data processing components included air pressure sensor within the air cylinder, electronic feedback system and monitors. The data obtained by the sensor are transmitted to an electronic feedback system through the external communication bus for data processing (Figure 1E). The processed data can be displayed in real time (Figure 1F).

2.4 | Ex-CMR protocol

The Ex-CMR protocol consisted of CMR scans during a 30-s baseline rest, a 5-min ramped exercise or to exhaustion and a 15-min recovery periods. The subject was placed supine in the MR bore with ECG patches on the chest. To do exercise stress, the subject placed both feet on a pair of pedals to perform a leg-stepping movement and an auditory beeping sound was provided through a headset to help the subject maintain the stepping frequency at 60 steps/min. The exercise protocol consisted of 5 min exercise at an average workload of 45 W. The work power was calculated based on the ideal gas law and the stepping frequency. During the entire Ex-CMR scans, heart rate and blood pressure were continuously measured by an MR-compatible physiological monitoring system.

CMR imaging was performed on a 3.0T clinical MR scanner (Skyra; Siemens Healthcare) with a phase-array surface coil. In this pilot study, myocardial native T1 and first-pass perfusion imaging were performed to study the rest-stress differences. Native T1 maps at mid-ventricular short-axis locations were acquired with free breathing using a MOLLI 5(3)3 sequence (MyoMaps; Siemens Healthcare) with inline motion-correction. Typical parameters included slice 8.0 mm thick, FOV 306 × 360 mm, flip angle 35°, minimum T1 120 ms, TI increment 80 ms, and acquisition time 14 s. Native T1 maps during the exercise stress were acquired at the first and third minute after the start of the exercise.

The first-pass perfusion imaging during the exercise was performed immediately after the second stress T1 imaging with a bolus injection of gadolinium (Gd) (gadopentetate dimeglumine) at a dose of 0.05 mL/kg body weight, followed by a saline flush with a power injector at a flow rate of 4 mL/s. The subjects were instructed to hold their breath after the start of the perfusion scan for approximately 20 s. Contrast agent passage was imaged by using a saturation-recovery Turbo fast low angle shot (turboFLASH) sequence provided by the vendor. The imaging parameters were as follows: TR/TE = 147.78 ms/0.99 ms; FOV = 260 × 337 mm²; matrix size: 108 × 192 mm²; flip angle = 10°; and 80 dynamics per slice. The saturation recovery time (from the saturation pulse to the middle of the readout) was

95 ms. Rest perfusion images were acquired 15 min after the exercise stress to allow sufficient time for clearance of the contrast agent. This Ex-CMR protocol took a total of 30 mins. In all subjects, a retest scan using the same Ex-CMR protocol was performed to assess test–retest reproducibility.

2.5 | Ex-CMR data analysis

All CMR images were reviewed offline by two independent experienced observers (Dr Gao and Dr Chen with 20 and 5 y of experience, respectively) blinded to the subject information to ensure that these images had sufficient diagnosis quality to be included for further analysis. Observers manually draw contours to outline the endocardium and epicardium on the native T1 maps using a commercially available cardiac software CVI⁴¹ (Version 5.3.2; Circle Cardiovascular Imaging). T1 reactivity was expressed in absolute terms: $\Delta T1(\text{ms}) = T1_{\text{stress}} - T1_{\text{rest}}$ and as percentages: $\delta T1(\%) = \Delta T1 \div T1_{\text{rest}} \times 100$.

For perfusion analysis, all perfusion images were first corrected for both respiratory and cardiac motion using a robust motion correction (MoCo) technique.¹⁹ The arterial input function was retrospectively corrected for the saturation effect using a model validated by perfusion measurements with positron emission tomography (PET).²⁰ Pixel-wide myocardial blood flow (MBF) maps at short-axis view were then created in mL/min/g at rest and during the exercise stress using a custom-made software.²¹ Myocardium in each map was divided into six segments and the mean MBF of each segment was obtained. The global MBF was calculated from the mean MBF of six segments at the mid-ventricular short-axis location. As resting MBF is determined by cardiac workload,¹³ we corrected resting MBF for the rate-pressure product (RPP), an index of myocardial oxygen consumption: Normalized MBF = $(\text{MBF}/\text{RPP}) \times 10^4$. MPR was defined as the ratio of stress MBF to rest MBF, and normalized MPR = $(\text{MPR}/\text{RPP}) \times 10^4$.

2.6 | Statistical analysis

Normality of the data was assessed using the Shapiro–Wilk test. Continuous normal data are expressed as mean \pm SD, and differences between rest and stress were analyzed with the two-sample *t*-test. Reliability (test–retest) and validity were assessed using the intraclass correlation coefficients (ICCs) to control for operator variance. Bland–Altman analysis and coefficient of variance (CoV) were also obtained. *P* values were considered statistically significant

when < 0.05 . Statistical analysis was performed using SPSS version 24 (IBM Corp).

3 | RESULTS

3.1 | MR compatibility testing

Inspection via a hand magnet demonstrated no perceptible magnetic attraction from any ergometer component individually or from the fully assembled device. There was no any indication that the presence of the ergometer device within the MR bore induces image artifacts and field inhomogeneity.

3.2 | Baseline characteristics of the subjects

All the subjects underwent the resting and exercise stress scans successfully without any premature termination of tests. The participants can perform sufficiently vigorous exercise without knee touching the inside surface of the scanner bore. One patient was excluded because the motion artifacts were not corrected adequately (Supporting Information Figure S1). The characteristics and hemodynamics of the 10 subjects are summarized in Table 1.

During the exercise test, the mean heart rate, systolic blood pressure, and RPP significantly increased with exercise (Figure 2). The peak heart rate was 136 ± 10 bpm, corresponding to $70 \pm 5\%$ of the age-predicted maximal heart rate (APMHR) in healthy subjects. The maximal RPP increased significantly by $121 \pm 33\%$. Between test and retest, there were strong agreement (intra-class correlation coefficient = 0.88 and 0.81, respectively) and good reproducibility (CoV = 6.10% and 6.16%, respectively) in the heart rates at the first and third minute during the exercise. Bland–Altman plots for stress heart rate, systolic blood pressure, and RPP from the two tests are shown in Figure 3.

3.3 | Changes in myocardial native T1 and perfusion during the exercise

Stress real-time native T1 and first-pass perfusion imaging were successfully completed in 10 subjects during the exercise. Compared with resting native T1 (1257 ± 38 ms), stress native T1 values increased significantly to 1301 ± 62 ms at first minute ($P < 0.05$) and 1319 ± 59 ms at third minute ($P < 0.05$) (Figure 2). During the stress, MBF increased significantly ($P < 0.05$) in

TABLE 1 General characteristics of the 10 healthy subjects

Variable	Value
Female, n (%)	5 (50%)
Age (y)	25.7 ± 1.8
BMI (kg/m ²)	21.6 ± 3.8
Height range (m)	1.52–1.83
Resting blood pressure (mm Hg)	
Systolic	113 ± 11
Diastolic	73 ± 9
Resting heart rate (beats/min)	72 ± 6
Resting RPP (beats/min × mm Hg)	8158 ± 1082
Stress systolic pressure during first minute (mm Hg)	142 ± 9
Stress diastolic pressure during first minute (mm Hg)	82 ± 8
Stress heart rate during first minute (beats/min)	125 ± 13
Stress RPP during first minute (beats/min × mm Hg)	17 814 ± 2181
Stress systolic pressure during third mins (mm Hg)	141 ± 12
Stress diastolic pressure during third mins (mm Hg)	80 ± 6
Stress heart rate during third mins (beats/min)	119 ± 3
Stress RPP during third mins (beats/min × mm Hg)	16 840 ± 2463
Recovery systolic pressure (mm Hg)	112 ± 13
Recovery diastolic pressure (mm Hg)	72 ± 9
Recovery heart rate (beats/min)	71 ± 6
Recovery RPP (beats/min × mm Hg)	7930 ± 1192

Note: Values are mean ± SD, n (%).

both test and retest (1.49 ± 0.30 and 1.59 ± 0.30 mL/min/g, respectively, Table 2) in comparison with the resting MBF (0.96 ± 0.29 and 0.96 ± 0.20 mL/min/g).

3.4 | Reproducibility of stress native T1 and perfusion

For the global exercise native T1 at the first and third minute, there was a strong agreement (intra-class correlation coefficient = 0.75 and 0.89, respectively) and excellent reproducibility (CoV = 3.05% and 2.02%, respectively, Table 2). Reproducibility between test and retest was good for stress global MBF (CoV = 10.7%, ICC = 0.84). The

variability of MPR was the lowest, represented by the highest ICC (0.92) and strong CoV values (8.8%). Mean values of MBF and MPR at rest and stress for both tests are shown in Table 2. Figure 3 shows the Bland–Altman plots in stress native T1 at the first and third minute, as well as stress MBF.

4 | DISCUSSION

This study demonstrates a new compact MR-compatible exercise device and examined its feasibility for Ex-CMR in terms of myocardial native T1 and MBF. The heart rate, systolic blood pressure, and RPP increased significantly during the exercise stress. Both myocardial native T1 and MBF increased significantly during the exercise stress in young healthy subjects. Furthermore, the reproducibility of measurement for native T1 is excellent and is good for stress MBF and MPR. The pilot testing demonstrated that this compact ergometer successfully induced cardiac stress for diagnosis purpose while simultaneously allowing high quality MR imaging during the exercise stress.

The present pedal ergometer uses an up/down pedal motion, which has the benefit of reduced upper body motion, thus reduced motion artifact in comparison with supine cycle ergometer. It is noted that the dimension of this equipment is relatively small, which is different from another similar commercial supine stepper.¹⁷ Furthermore, in comparison with the traditional equipment that provides only a limited number of resistance adjustments,¹⁷ this equipment has a variety of workload that can be adjusted tailored to the imaging protocol and the need of individual subjects.

Given the relatively narrow bore diameter in MR scanners (approx. 70 cm), some typical limitations with bicycle-style ergometers are that tall participants would not be able to achieve a sufficient level of supine exercise²² and it may be difficult to establish a steady state workload.²³ Pedal ergometer in this study overcame the above limitations. With the help of adjusting the patient flat (lying) body position and knee height, participant's knee did not hit/touch the inside of the magnet bore during the vigorous pedaling. In addition, unlike the previous similar commercially available device which is often used for skeletal muscle exercise testing,^{24,25} our equipment can accomplish other exercise tasks (e.g., isometric exercise) for organs such as the thigh, the calf, and the feet.

Perhaps the most significant finding is the heart rate in current study increased by 74%, which is similar to $70 \pm 5\%$ of the APMHR. This finding differs from that of Thomas et al. (2020) who showed that it is more difficult to reach the maximal heart rate with supine exercise than with upright exercise.²⁶ Previous studies have shown

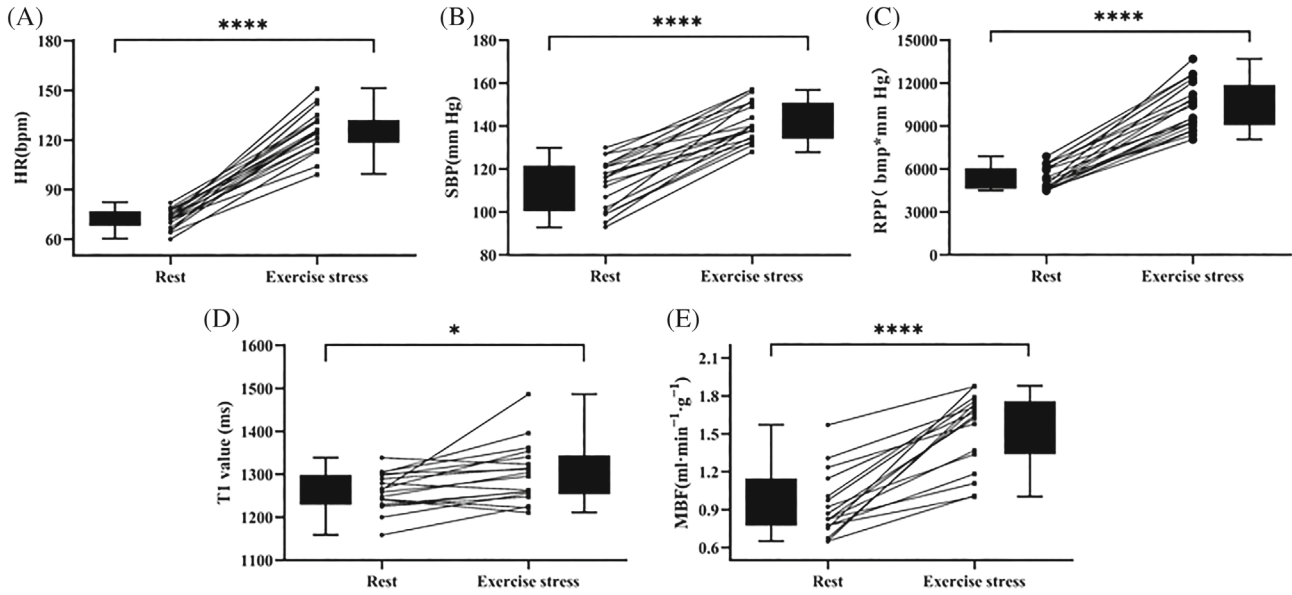


FIGURE 2 The effects on heart rate (HR) (A), systolic blood pressure (SBP) (B), RPP (C), native T1 (D), and MBF (F) in all subjects underwent the Ex-CMR. All mean values of the respective parameters increased significantly during the exercise stress, compared to counterparts at rest.

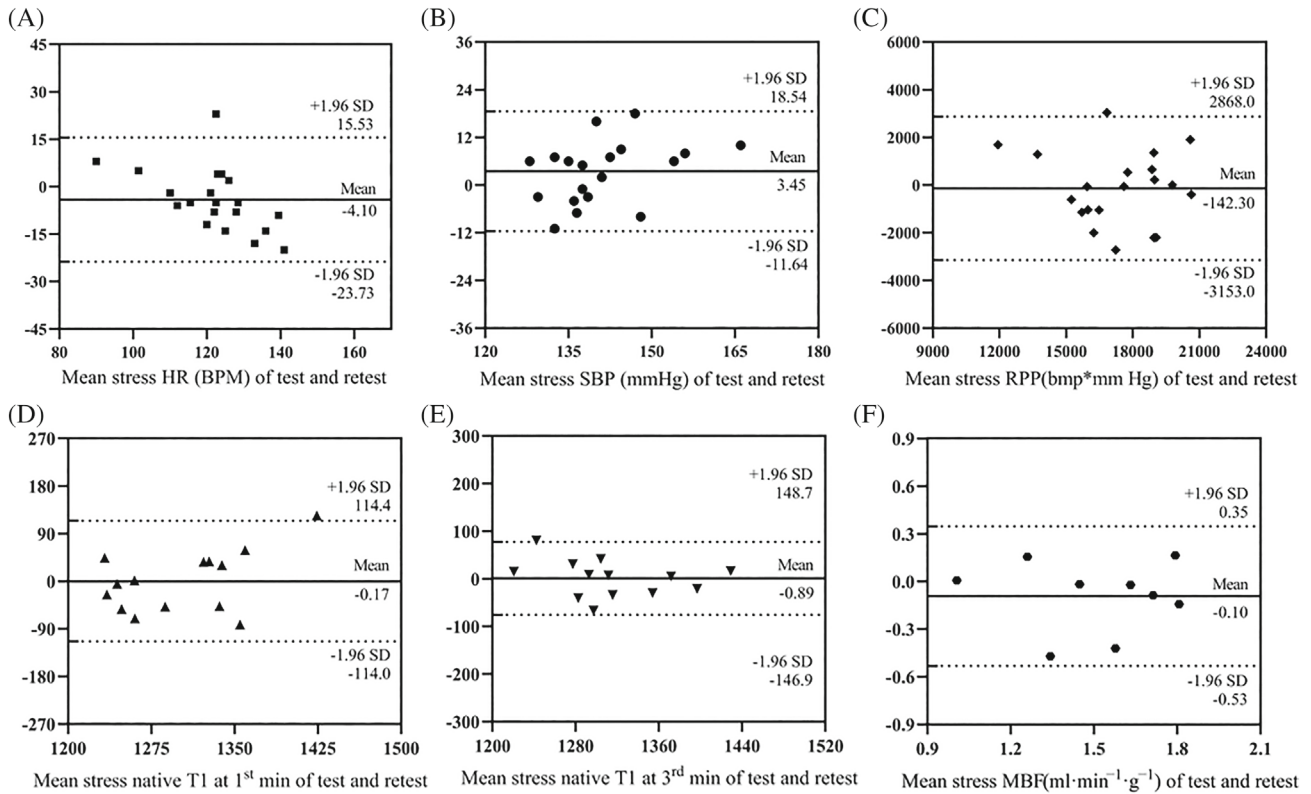


FIGURE 3 The Bland–Altman plots. Test–retest reproducibility of heart rate (HR) (A), systolic blood pressure (SBP) (B), RPP (C), and native T1 using exercise stress with motion correction in all healthy young subjects at first (D) and third (E) minute and stress MBF (F).

a couple of reasons. First, compared with upright exercise, supine exercise can lead to muscle fatigue more quickly and can strongly reduce the musculature of the recruited

lower extremities.²⁷ Second, supine exercise may raise systolic blood pressure much higher than upright exercise does, thus resulting in similar increases like in RPP.^{10,28}

TABLE 2 Reproducibility of rest and stress native T1 and myocardial blood flows

Parameter	Test 1	Test 2	CoV (%)	ICC (95% CI)	P value
Global T1					
Rest	1248 (34)	1266 (42)	1.68	0.87 (0.57; 0.96)	0.001**
Stress 1 min	1302 (76)	1302 (51)	3.05	0.75 (0.22; 0.92)	0.009**
Stress 3 min	1316 (57)	1314 (67)	2.02	0.89 (0.64; 0.97)	0.001**
Recovery	1057 (50)	1042 (27)	2.84	0.62 (−0.67; 0.92)	0.095
Global perfusion					
Rest MBF	0.96 (0.29)	0.96 (0.20)	15.13	0.77 (−0.02; 0.95)	0.027*
Normalized Rest MBF	1.15 (0.30)	1.20 (0.26)	13.88	0.77 (0.00; 0.95)	0.025*
Stress MBF	1.49 (0.30)	1.59 (0.30)	10.70	0.84 (0.28; 0.96)	0.010*
Normalized stress MBF	0.94 (0.10)	0.99 (0.14)	9.39	0.66 (−0.69; 0.93)	0.087
MPR	1.69 (0.45)	1.72 (0.41)	8.80	0.92 (0.68; 0.98)	0.001**
Normalized MPR	1.32 (0.28)	1.35 (0.21)	8.35	0.87 (0.39; 0.98)	0.006**

* $P < 0.05$.** $P < 0.01$.

Like multiple exercise studies have reported,²⁹ our exercise intensity reached its sub-maximum. The increased heart rate and RPP are consistent with recent observations by another study that used Lode BV (Up/Down) ergometer in which image acquisition is at moderate workload intensities.³⁰ Hence, it could be possible to perform the pedal ergometer to maximal intensity heart rates by increasing the workload intensities or exercise time.

Exercise has been recognized as the most important efficient physiological stimulus that increases the demand on myocardial oxygen.³¹ Limited studies have demonstrated similar physiological responses between exercise and dobutamine induced stress, in terms of increased heart rate, blood flow, and oxygen demand.¹² The results of this study are in accord with a previous study reporting that the hemodynamic responses of healthy controls to dobutamine stress were similar to those to physical exercise tests.³² Sundin et al.³³ administered a dobutamine dose of $22 \pm 6 \mu\text{g}/\text{kg}/\text{min}$, which increased heart rate by 64% and increased systolic blood pressure by 14%. The increase in heart rate obtained in our study (74%) is in line with these results with pharmacological stress. Nevertheless, whether our compact ergometer permits accurate and reliable assessment of biventricular function remains to be studied in a clinical setting.³⁴

Dobutamine stress leads to MRP of 1.73 ± 0.73 to 1.97 ± 1.13 , which is comparable to our MPR of 1.69 ± 0.45 or 1.72 ± 0.41 during the exercise.³⁵ Our results of exercise stress MBF and MPR regarding healthy subjects were comparable to those observed with intravenous dobutamine or other maximal exercise on a treadmill protocol in CMR.^{35,36} In addition, the T1 reactivity seems to

show better reproducibility (lower CoV%) compared to MBF and MPR measurements. The CoV of T1 mapping during stress in our study (3.05% or 2.02%) is in line with the results reported by Federica et al, in which the test–retest reliability was from good to excellent for stress native T1(1.5%).³⁷ Test–retest reliability of MPR of this study (8.8%) is also in accord with other studies reporting that the CoV value of test–retest reliability of MPR was from 13.3% to 35%^{38,39} in healthy subjects and ICCs varied from 0.26 to 0.88.^{39,40} Although the specific reasons for less reproducibility in MBF and MPR measurement are unknown, the residual motion artifacts, errors in AIF estimation, and/or physiology difference of participants at two different days may all contribute to this slightly poorer reproducibility.

It is noted the exercise stress augmented native T1 by using this compact ergometer. Several studies have revealed that native (non-contrast) T1 mapping may be used to quantify myocardial water content^{41–43} and the T1 reactivity can differentiate between normal, infarcted, ischemic, and remote myocardium with distinctive T1 profiles, thus holding promise for ischemia detection without the need for gadolinium contrast injections.^{42,44,45} In this pilot study, exercise stress and the change in myocardial T1 during stress (T1 reactivity = 4.9%) are similar to previous adenosine and exercise stress T1-mapping studies.^{32,44,46,47}

5 | LIMITATIONS

There are several limitations in this pilot study. First, the sample size is very limited, and no cardiac patients

were involved in the tests. Second, this study lacks direct comparison with perfusion imaging with pharmaceutically induced stress in the present study. It would be interesting to compare these two types of stress mechanisms in terms of their effectiveness for the diagnosis of coronary artery disease. Third, the subjects were not instructed to abstain from vigorous exercise and caffeine/tea consumption prior to each visit, which may affect MBF values. Finally, our findings with regards to the moderate reproducibility in MBF and MPR may reflect residual exercise motion artifacts during stress. Consequently, more technical developmental work in Ex-CMR acquisition methods such as 3D perfusion and T1 mapping sequences with motion correction, need to be done prior to using this compact ergometer in routine clinical study of cardiac patients.

In conclusion, we designed, constructed, and examined an MR-compatible compact ergometer for Ex-CMR within the MR bore. The increases in heart rate and RPP during the moderate exercise are similar to those by using dobutamine stress. The reproducibility of native T1, MBF, and MPR measurements during the exercise stress are from good to excellent. More studies are necessary to examine the diagnosis utility with this compact ergometer in a variety of cardiovascular diseases.

ACKNOWLEDGMENTS

We appreciate Yue Jiang's assistance with the linguistic editing and proofreading of this manuscript. We also thank Ruoyang Li, Haichen Li and Haotian Chen for their assistance with the data acquisition. This study was supported in part by the National Natural Science Foundation of China (No. 81930046 and 81829003) and The Expert Workstation of Yunnan Province (No. 202105AF150037), as well as by the Department of Radiology, Medical Imaging of West China Hospital, Sichuan University, Chengdu, Sichuan, China.

ORCID

Yang Yang  <https://orcid.org/0000-0002-2841-4243>

Fabao Gao  <https://orcid.org/0000-0003-2257-3275>

REFERENCES

- Baumgartner H, Falk V, Bax JJ, et al. 2017 ESC/EACTS guidelines for the management of valvular heart disease. *Eur Heart J*. 2017;38:2739-2791.
- Stout KK, Daniels CJ, Aboulhosn JA, et al. 2018 AHA/ACC guideline for the Management of Adults with Congenital Heart Disease: executive summary: a report of the American College of Cardiology/American Heart Association task force on clinical practice guidelines. *J Am Coll Cardiol*. 2019;73:1494-1563.
- Knott KD, Seraphim A, Augusto JB, et al. The prognostic significance of quantitative myocardial perfusion: an artificial intelligence-based approach using perfusion mapping. *Circulation Apr 21*. 2020;141:1282-1291.
- Rahman H, Ryan M, Lumley M, et al. Coronary microvascular dysfunction is associated with myocardial ischemia and abnormal coronary perfusion during exercise. *Circulation*. 2019;140:1805-1816.
- Le TT, Bryant JA, Ting AE, et al. Assessing exercise cardiac reserve using real-time cardiovascular magnetic resonance. *J Cardiovasc Magn Reson*. 2017;19:7.
- Gibbons RJ, Balady GJ, Bricker JT, et al. ACC/AHA 2002 guideline update for exercise testing: summary article. A report of the American College of Cardiology/American Heart Association task force on practice guidelines (committee to update the 1997 exercise testing guidelines). *J Am Coll Cardiol*. 2002;40:1531-1540.
- Arnold JR, McCann GP. Cardiovascular magnetic resonance: applications and practical considerations for the general cardiologist. *Heart*. 2020;106:174-181.
- Kramer CM, Barkhausen J, Bucciarelli-Ducci C, Flamm SD, Kim RJ, Nagel E. Standardized cardiovascular magnetic resonance imaging (CMR) protocols: 2020 update. *J Cardiovasc Magn Reson*. 2020;22:17.
- Lancellotti P, Pellikka PA, Budts W, et al. The clinical use of stress echocardiography in non-Ischaemic heart disease: recommendations from the European Association of Cardiovascular Imaging and the American Society of Echocardiography. *J Am Soc Echocardiogr*. 2017;30:101-138.
- Craven TP, Jex N, Chew PG, et al. Exercise cardiovascular magnetic resonance: feasibility and development of biventricular function and great vessel flow assessment, during continuous exercise accelerated by compressed SENSE: preliminary results in healthy volunteers. *Int J Cardiovasc Imaging*. 2021;37:685-698.
- Wolk MJ, Bailey SR, Doherty JU, et al. ACCF/AHA/ASE/ASNC/HFSA/HRS/SCAI/SCCT/SCMR/STS 2013 multimodality appropriate use criteria for the detection and risk assessment of stable ischemic heart disease: a report of the American College of Cardiology Foundation appropriate use criteria task force, American Heart Association, American Society of Echocardiography, American Society of Nuclear Cardiology, Heart Failure Society of America, Heart Rhythm Society, Society for Cardiovascular Angiography and Interventions, Society of Cardiovascular Computed Tomography, Society for Cardiovascular Magnetic Resonance, and Society of Thoracic Surgeons. *J Am Coll Cardiol*. 2014;63:380-406.
- Fletcher GF, Ades PA, Kligfield P, et al. Exercise standards for testing and training: a scientific statement from the American Heart Association. *Circulation*. 2013;128:873-934.
- Raman SV, Dickerson JA, Jekic M, et al. Real-time cine and myocardial perfusion with treadmill exercise stress cardiovascular magnetic resonance in patients referred for stress SPECT. *J Cardiovasc Magn Reson*. 2010;12:41.
- Foster EL, Arnold JW, Jekic M, et al. MR-compatible treadmill for exercise stress cardiac magnetic resonance imaging. *Magn Reson Med*. 2012;67:880-889.
- Raman SV, Dickerson JA, Mazur W, et al. Diagnostic performance of treadmill exercise cardiac magnetic resonance: the prospective, multicenter exercise CMR's accuracy for cardiovascular stress testing (EXACT) trial. *J Am Heart Assoc*. 2016;5:e003811.

16. Lurz P, Muthurangu V, Schuler PK, et al. Impact of reduction in right ventricular pressure and/or volume overload by percutaneous pulmonary valve implantation on biventricular response to exercise: an exercise stress real-time CMR study. *Eur Heart J*. 2012;33:2434-2441.
17. Forouzan O, Flink E, Warczytowa J, et al. Low cost magnetic resonance imaging-compatible stepper exercise device for use in cardiac stress tests. *J Med Device*. 2014;8:0450021-0450028.
18. La Gerche A, Claessen G, Van de Bruaene A, et al. Cardiac MRI: a new gold standard for ventricular volume quantification during high-intensity exercise. *Circ Cardiovasc Imaging*. 2013;6:329-338.
19. Xue H, Shah S, Greiser A, et al. Motion correction for myocardial T1 mapping using image registration with synthetic image estimation. *Magn Reson Med*. 2012;67:1644-1655.
20. Edalati M, Muccigrosso D, Laforest R, et al. Correlations and differences of myocardial blood flow with simultaneous measurements of MRI and PET. *Proceeding of Annual Conference of ISMRM*. Hawaii; 2017:0534.
21. Goldstein TA, Zhang H, Misselwitz B, Gropler RG, Zheng J. Improvement of quantification of myocardial first-pass perfusion mapping: a temporal and spatial wavelet denoising method. *Magn Reson Med*. 2006;56:439-445.
22. Pflugi S, Roujol S, Akçakaya M, et al. Accelerated cardiac MR stress perfusion with radial sampling after physical exercise with an MR-compatible supine bicycle ergometer. *Magn Reson Med*. 2015;74:384-395.
23. Gusso S, Salvador C, Hofman P, et al. Design and testing of an MRI-compatible cycle ergometer for non-invasive cardiac assessments during exercise. *Biomed Eng Online*. 2012;11:13.
24. Valkovič L, Chmelík M, Ukropcová B, et al. Skeletal muscle alkaline pi pool is decreased in overweight-to-obese sedentary subjects and relates to mitochondrial capacity and phosphodiester content. *Sci Rep*. 2016;6:20087.
25. Ergospect. <https://ergospect.com/cardio-step-module/>
26. Craven TP, Tsao CW, La Gerche A, Simonetti OP, Greenwood JP. Exercise cardiovascular magnetic resonance: development, current utility and future applications. *J Cardiovasc Magn Reson*. 2020;22:65.
27. Dillon HT, Dausin C, Claessen G, et al. The effect of posture on maximal oxygen uptake in active healthy individuals. *Eur J Appl Physiol*. 2021;121:1487-1498.
28. Chew PG, Swoboda PP, Ferguson C, et al. Feasibility and reproducibility of a cardiovascular magnetic resonance free-breathing, multi-shot, navigated image acquisition technique for ventricular volume quantification during continuous exercise. *Quant Imaging Med Surg*. 2020;10:1837-1851.
29. Beaudry RI, Samuel TJ, Wang J, Tucker WJ, Haykowsky MJ, Nelson MD. Exercise cardiac magnetic resonance imaging: a feasibility study and meta-analysis. *Am J Physiol Regul Integr Comp Physiol*. 2018;315:R638-r645.
30. Barber NJ, Ako EO, Kowalik GT, et al. Magnetic resonance-augmented cardiopulmonary exercise testing: comprehensively assessing exercise intolerance in children with cardiovascular disease. *Circ Cardiovasc Imaging*. 2016;9:e005282.
31. Duncker DJ, Bache RJ. Regulation of coronary blood flow during exercise. *Physiol Rev*. 2008;88:1009-1086.
32. Oosterhof T, Tulevski II, Roest AA, et al. Disparity between dobutamine stress and physical exercise magnetic resonance imaging in patients with an intra-atrial correction for transposition of the great arteries. *J Cardiovasc Magn Reson*. 2005;7:383-389.
33. Sundin J, Engvall J, Nylander E, Ebberts T, Bolger AF, Carlhäll CJ. Improved efficiency of intraventricular blood flow transit under cardiac stress: a 4D flow Dobutamine CMR study. *Front Cardiovasc Med*. 2020;7:581495.
34. Vasu S, Little WC, Morgan TM, et al. Mechanism of decreased sensitivity of dobutamine associated left ventricular wall motion analyses for appreciating inducible ischemia in older adults. *J Cardiovasc Magn Reson*. 2015;17:26.
35. Miller CA, Naish JH, Ainslie MP, et al. Voxel-wise quantification of myocardial blood flow with cardiovascular magnetic resonance: effect of variations in methodology and validation with positron emission tomography. *J Cardiovasc Magn Reson*. 2014;16:11.
36. Jekic M, Foster EL, Ballinger MR, Raman SV, Simonetti OP. Cardiac function and myocardial perfusion immediately following maximal treadmill exercise inside the MRI room. *J Cardiovasc Magn Reson*. 2008;10:3.
37. Poli FE, Gulsin GS, March DS, et al. The reliability and feasibility of non-contrast adenosine stress cardiovascular magnetic resonance T1 mapping in patients on haemodialysis. *J Cardiovasc Magn Reson*. 2020;22:43.
38. Larghat AM, Maredia N, Biglands J, et al. Reproducibility of first-pass cardiovascular magnetic resonance myocardial perfusion. *J Magn Reson Imaging*. 2013;37:865-874.
39. Brown LAE, Onciul SC, Broadbent DA, et al. Fully automated, inline quantification of myocardial blood flow with cardiovascular magnetic resonance: repeatability of measurements in healthy subjects. *J Cardiovasc Magn Reson*. 2018;20:48.
40. Likhite D, Suksaranjit P, Adluru G, et al. Interstudy repeatability of self-gated quantitative myocardial perfusion MRI. *J Magn Reson Imaging*. 2016;43:1369-1378.
41. Kuijpers D, Prakken NH, Vliegenthart R, van Dijkman PR, van der Harst P, Oudkerk M. Caffeine intake inverts the effect of adenosine on myocardial perfusion during stress as measured by T1 mapping. *Int J Cardiovasc Imaging*. 2016;32:1545-1553.
42. Nickander J, Themudo R, Thalen S, et al. The relative contributions of myocardial perfusion, blood volume and extracellular volume to native T1 and native T2 at rest and during adenosine stress in normal physiology. *J Cardiovasc Magn Reson*. 2019;21:73.
43. Liu A, Wijesurendra RS, Francis JM, et al. Adenosine stress and rest T1 mapping can differentiate between ischemic, infarcted, remote, and Normal myocardium without the need for gadolinium contrast agents. *JACC Cardiovasc Imaging*. 2016; 9:27-36.
44. Piechnik SK, Neubauer S, Ferreira VM. State-of-the-art review: stress T1 mapping-technical considerations, pitfalls and emerging clinical applications. *Magma*. 2018;31:131-141.
45. Burrage MK, Shanmuganathan M, Zhang Q, et al. Cardiac stress T1-mapping response and extracellular volume stability of MOLLI-based T1-mapping methods. *Sci Rep*. 2021;11:13568.
46. Nakamori S, Fahmy A, Jang J, et al. Changes in myocardial native T(1) and T(2) after exercise stress: a noncontrast CMR pilot study. *JACC Cardiovasc Imaging*. 2020;13:667-680.
47. Bohnen S, Prüßner L, Vettorazzi E, et al. Stress T1-mapping cardiovascular magnetic resonance imaging and inducible myocardial ischemia. *Clin Res Cardiol*. 2019;108:909-920.

SUPPORTING INFORMATION

Additional supporting information may be found in the online version of the article at the publisher's website.

Figure S1 The first-pass perfusion images for the subject that was excluded due to poor MoCo. The first-pass perfusion image captured in frame 8 is in systole, whereas the one in frame 9 is in diastole. This represents difficult-to-correct nonrigid motion. Also, the deep breathing-pattern typically seen during exercise stress is

visualized in frames 10–15 (large through-plane motion which is difficult for MoCo to correct).

How to cite this article: He B, Chen Y, Wang L, et al. Compact MR-compatible ergometer and its application in cardiac MR under exercise stress: A preliminary study. *Magn Reson Med*.

2022;88:1927-1936. doi: 10.1002/mrm.29311